Monomeric Titanium(IV) Azides as a New Route to Titanium Nitride

Claire J. Carmalt,[†] Alan H. Cowley,*[,†] Robert D. Culp,[†] Richard A. Jones,*[,†] Yang-Ming Sun,[‡] Bill Fitts,[‡] Sandra Whaley,[‡] and Herbert W. Roesky[§]

Department of Chemistry & Biochemistry, The University of Texas at Austin, Austin, Texas 78712, Center for Materials Chemistry, The University of Texas at Austin, Austin, Texas 78712, and Institut für Anorganische Chemie der Universität, Tammannstrasse 4, D-37077, Göttingen, Germany

Received December 12, 1996[⊗]

The reaction of $Ti(NMe_2)_4$ with 2 equiv of Me_3SiN_3 in toluene solution affords a dark red polymeric material of composition $[Ti(NMe_2)_2(N_3)_2]_n$ (**1**). If the reaction is carried out in pyridine (py) solution, dark red, crystalline $[Ti(NMe_2)_2(N_3)_2(py)_2]$ (**2**) is formed. Analogous reactions of $Ti(NMe_2)_4$ with 2 or 1 equiv of Me_3SiN_3 in the presence of 1 equiv of bipyridyl (bipy) in toluene solution afford brown crystals of $[Ti(NMe_2)_2(N_3)_2(bipy)]$ (**3**) and dark red crystals of $[Ti(NMe_2)_3(N_3)(bipy)]$ (**4**), respectively. Crystallographic data for **2**: orthorhombic, $C222_1$, $a = 7.120(1)$ Å, $b = 15.899(3)$ Å, $c = 16.946(4)$ Å, $V = 1918.3(6)$ Å^3, $\rho = 1.310$ g/cm^3, $Z = 4$. Crystallographic data for **3**: monoclinic, $I2/a$, $a = 7.358(2)$ Å, $b = 16.808(4)$ Å, $c = 14.837(6)$ Å, $\beta = 95.40(2)°$, $V = 1826.8(1)$ Å^3, $\rho = 1.368$ g/cm^3, $Z = 4$. Crystallographic data for **4**: monoclinic, $P2_1/c$, $a = 15.682(2)$ Å, $b = 8.814(1)$ Å, $c = 15.128(1)$ Å, $\beta = 108.39(1)°$, $V = 1984.2(4)$ Å^3, $\rho = 1.267$ g/cm^3, $Z = 4$. Compounds **1** and **2** deposit thin films of titanium nitride (TiN) on silica and/or nickel substrates in the temperature range 300−400 °C. The TiN films deposited from precursor **2** are superior to those deposited from **1**.

Introduction

The high metallic conductivity and refractory nature of transition metal nitrides render these materials well suited for service as diffusion barriers in a variety of metallization structures of advanced microelectronic devices.[1,2] Of the several transition metal nitrides, titanium nitride (TiN) is used the most extensively because, in addition to low resistivity and excellent thermal stability, this material exhibits good conformality and high tolerance to chemical etching.[1]

The traditional preparation of TiN involves the thermal reaction of NH_3 with either $TiCl_4$[3] or $Ti(NMe_2)_4$.[4] Significant problems have arisen, however, with both synthetic methods.[5] Thus the $TiCl_4$ route, while resulting in excellent step coverage, requires undesirably high reaction temperatures and the deposited TiN films feature potentially corrosive chlorine contamination. On the other hand, the use of $Ti(NMe_2)_4$ as the titanium source results in poor step coverage. Interestingly, however, acceptable step coverage can be achieved by using $Ti(NEt_2)_4$ in place of $Ti(NMe_2)_4$.[6]

In an effort to address some of the foregoing problems and to find a low-temperature, high growth rate synthesis of TiN, several single-source TiN precursors have been synthesized and employed in deposition studies. The list includes $Ti(NR_2)_4$ (R = Me, Et),[7] $[Ti(NMe_2)_3(t\text{-Bu})]$,[7] $[Ti(\mu\text{-N-}t\text{-Bu})(NMe_2)_2]_2$,[7] $[CpTiCl_2\{N(SiMe_3)_2\}]$,[8] $[Cp_2Ti(N_3)_2]$,[9] $[TiCl_2(NH\text{-}t\text{-Bu})_2(NH_2\text{-}t\text{-Bu})_2]_n$,[10] and $[TiCl_4(NH_3)_2]$.[11] However, the volatility of the oligomeric species was found to be very low and the use of precursors with Ti−C or Ti−Cl bonds resulted in carbon and chlorine contamination, respectively. Moreover, the use of $[CpTiCl_2\{N(SiMe_3)_2\}]$[8] and $[Cp_2Ti(N_3)_2]$[9] resulted in the formation of titanium carbonitride rather than titanium nitride. Guided by our previous work on a successful gallium nitride (GaN) precursor, $[Ga(NMe_2)(N_3)(\mu\text{-}NMe_2)]_2$,[12] we decided to explore the possibility of preparing TiN precursors with potentially labile amido groups and azide nitrogen delivery moieties. It was anticipated that, in order to isolate monomeric derivatives, it would be necessary to introduce N-donor ligands into the coordination sphere. Previous experience with gallium azides indicated that pyridine (py) would be the ligand of choice.[13] However, bipyridine (bipy) was also investigated since the use of this ligand often results in crystalline derivatives.

Results and Discussion

Initial attempts to prepare azido derivatives of $Ti(NMe_2)_4$ involved the addition of 2 equiv of Me_3SiN_3 to a toluene solution of $Ti(NMe_2)_4$ at room temperature. An immediate color change from yellow to blood red was observed and workup of the reaction mixture afforded a dark red solid. Combustion analysis and mass spectral data were consistent with the formation of a complex of formula $[Ti(NMe_2)_2(N_3)_2]_n$ (**1**), which is presumed to be polymeric on account of its low volatility and insolubility.

[†] Department of Chemistry & Biochemistry, The University of Texas.
[‡] Center for Materials Chemistry, The University of Texas.
[§] Institut für Anorganische Chemie der Universität.
[⊗] Abstract published in *Advance ACS Abstracts*, June 1, 1997.

(1) Oyama, S. T. *The Chemistry of Transition Metal Carbides and Nitrides*; Blackie Academic & Professional: London, 1996.
(2) Pogger, H. B. *Electronic Materials Chemistry*; Marcel Dekker, Inc.: New York, 1996; and references therein.
(3) Kurtz, S. R.; Gordon, R. G. *Thin Solid Films* **1986**, *140*, 277.
(4) Fix, R. M.; Gordon, R. G.; Hoffman, D. M. *Chem. Mater.* **1991**, *3*, 1138 and references therein.
(5) Hoffman, D. M. *Polyhedron* **1994**, *13*, 1169 and references therein.
(6) Raaijmakers, I. J. *Thin Films Solids* **1994**, *247*, 85.
(7) Fix, R. M.; Gordon, R. G.; Hoffman, D. M. *Chem. Mater.* **1990**, *2*, 235 and references therein.
(8) Laurent, F.; Zhao, J. S.; Valade, L.; Choukroun, R.; Cassoux, P. *J. Anal. Appl. Pyrolysis* **1992**, *24*, 39.
(9) Ikeda, K.; Maeda, M.; Arita, Y. *Jpn. J. Appl. Phys.* **1993**, *32*, 3085.
(10) Winter, C. H.; Sheridan, P. H.; Lewkebandara, T. S.; Heeg, M. J.; Proscia, J. W. *J. Am. Chem. Soc.* **1992**, *114*, 1095. Lewkebandara, T. S.; Sheridan, P. H.; Heeg, M. J.; Rheingold, A. L.; Winter, C. H. *Inorg. Chem.* **1994**, *33*, 5879.
(11) Winter, C. H.; Lewkebandara, T. S.; Proscia, J. W.; Rheingold, A. L. *Inorg. Chem.* **1994**, *33*, 1227.
(12) Neumayer, D. A.; Cowley, A. H.; Decken, A.; Jones, R. A.; Lakhotia, V.; Ekerdt, J. G. *J. Am. Chem. Soc.* **1995**, *117*, 5893.
(13) Carmalt, C. J.; Cowley, A. H.; Culp, R. D.; Jones, R. A. *J. Chem. Soc., Chem. Commun.* **1996**, 1453.

S0020-1669(96)01483-8 CCC: $14.00

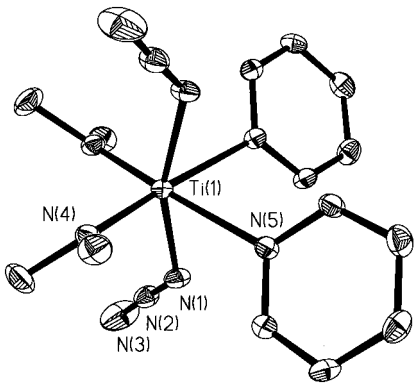

Figure 1. Molecular structure of $[Ti(NMe_2)_2(N_3)_2(py)_2]$ (**2**), showing the atom-numbering scheme. Ellipsoids are drawn at the 30% level. Hydrogen atoms are omitted.

Scheme 1

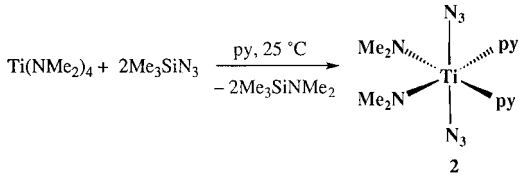

It is interesting to note that a previously reported reaction between $Ti(NMe_2)_4$ and 1 equiv of Me_3SiN_3 in benzene solution at ~5 °C resulted in the formation of a trimeric species with composition $[Ti(NMe_2)(N_3)(\mu\text{-}NMe_2)]_3(\mu_3\text{-}N_3)(\mu_3\text{-}NH)$.[14] Although the origin of the imido hydrogen was not established, it presumably arose from traces of moisture.

With a view to developing a mononuclear and more tractable TiN precursor, it was decided to attempt the depolymerization of **1** by reaction with an N-donor ligand. Accordingly, $Ti(NMe_2)_4$ was treated with 2 equiv of Me_3SiN_3 in the presence of an excess of pyridine (py) at room temperature (Scheme 1). A dark red crystalline product was obtained in 70% yield by diffusion of an overlayer of hexanes into the pyridine solution at −20 °C. Analytical and spectroscopic data were consonant with the empirical formulation $[Ti(NMe_2)_2(N_3)_2(py)_2]$ (**2**), and an X-ray crystallographic study revealed that the solid-state structure of **2** comprises monomeric units, one of which is depicted in Figure 1; selected bond lengths and angles are presented in Table 1. Compound **2** crystallizes in the orthorhombic space group $C222_1$. Individual molecules reside on a crystallographic C_2 axis, and there are no unusually short intermolecular contacts. The geometry about the titanium center is approximately octahedral, and the stereochemistry is such that the two azide ligands are situated *trans* to each other while the pyridine and dimethylamido ligands adopt mutually *cis* dispositions. The bond angles between the two amide groups and azide groups are ~98° and thus much wider than the ideal *cis* octahedral angle of 90°. Moreover, the *trans*-azides are arranged in a distinctly nonlinear fashion [N(1)−Ti(1)−N(1a) 161.30(2)°]. However, these deviations from the ideal octahedral angles are not particularly surprising given the different steric demands of the NMe_2 and azide groups. The Ti−N(pyridine) bond distances are not unusual for σ-donor interactions of this type;[15] the N(py)−Ti−N(py) angle is relatively acute [82.5(2)°]. The metrical parameters for the azide moieties are typical of those reported for a variety of covalent azides both in terms of the N−N−N bond angle [177.50(4)°] and also with respect to the observation of two significantly different N−N bond distances [1.183(4) and 1.135(5) Å].[16] Both azide groups point toward the least sterically hindered part of the molecule, *viz*. over the amide ligands. The Ti−N_3 bond distances of 2.075(3) Å in **2** are slightly longer than those in $[(C_5H_5)_2Ti(N_3)_2]$[17] (av. Ti−N_3 2.03 Å) and $[(C_6H_5)_4As]_2[TiCl_4(N_3)_2]$[18] (av. Ti−$N_3$ 2.01 Å), both of which possess terminal azido ligands. However, as expected, the foregoing Ti−N bond distances are shorter than those reported for bridging azide ligands, e.g. $[TiCl_3N_3]$[19] (av. Ti−N_3 2.105 Å), $[(C_6H_5)_4As]_2[TiCl_4N_3]_2$[20] (av. Ti−$N_3$ 2.116 Å), and $[(MeC_5H_4)TiCl_2N_3]_2$[21] [av. Ti−N_3 2.134 Å]. The Ti−NMe_2 bond distances of 1.901(3) Å are similar to those found in related amido complexes such as $[(Me_2N)_2Ti(\mu\text{-N-}t\text{-Bu})]_2$ (av. Ti−NMe_2 1.914 Å).[22]

Treatment of $Ti(NMe_2)_4$ with an equimolar quantity of bipyridine (bipy) in toluene solution, followed by the addition of 2 equiv of Me_3SiN_3, resulted, after workup, in a 55% yield of brown, crystalline **3** (Scheme 2). Combustion analysis and NMR data (^1H and $^{13}C\{^1H\}$) for **3** were consistent with the empirical composition $[Ti(NMe_2)_2(N_3)_2(bipy)]$. However, in order to establish both the degree of oligomerization and the stereochemistry at titanium it was necessary to appeal to X-ray crystallography. Compound **3** crystallizes in the monoclinic space group $I2/a$, and the solid state comprises an array of monomeric units, each of which resides on a crystallographic C_2 axis (Figure 2). There are no unusually short contacts between individual molecules; a selection of bond lengths and angles appears in Table 1. The molecular geometry of **3** is similar to that of **2** in the sense that pairs of azide and dimethylamido ligands are arranged in mutually *trans* and *cis* fashions, respectively. Perforce, the bipyridyl ligand occupies the two remaining *cis* sites of the approximately octahedral geometry at titanium. Due to the "bite" of the bipyridyl ligand, the N(5)−Ti−N(5a) bond angle is only 71.1(2)° and, as a consequence, the remaining bond angles depart commensurately from the ideal values: 99.9(3)° for N(4)−Ti−N(4a) and 165.2(3)° for N(1)−Ti−N(1a). The Ti−NMe_2 and Ti−N_3 bond lengths in **3** (1.906(5) and 2.067(5) Å, respectively) and the metrical parameters for the azide moieties are identical to those in **2** within experimental error; hence, the discussion of these aspects presented above for **2** is also applicable to **3**. The observation that the Ti−bipy bond length in **3** (2.274(5) Å) is shorter than the Ti−py bond length in **2** (2.311(3) Å) stems from the chelate effect. Finally, it is interesting to note that, whereas the azide groups in **2** point toward the amide ligands, these groups are located over the bipyridyl ligand in **3**. This conformational difference probably originates from the fact that, in contrast to the pyridine ligands, the bipyridyl ligands presents a planar face to the azide groups.

The use of 1 rather than 2 equiv of Me_3SiN_3 in the procedure described above for **3** resulted in a 60% yield of a red crystalline product, **4**, following workup. Collectively, the elemental analysis and $^1H/^{13}C\{^1H\}$NMR data were indicative of the empirical formulation $[Ti(NMe_2)_3(N_3)(bipy)]$ for **4**. Confirmation of this assignment was forthcoming from an X-ray analysis

(14) Gross, M. E.; Siegrist, T. *Inorg. Chem.* **1992**, *31*, 4898.
(15) Collier, P. E.; Dunn, S. C.; Mountford, P.; Shishkin, O. V.; Swallow, D. *J. Chem. Soc., Dalton Trans* **1995**, 3743.
(16) For a recent review on covalent azides, see: Tornieporth-Oetting, I. C.; Klapotke, T. M. *Angew. Chem., Int. Ed. Engl.* **1995**, *34*, 511.
(17) De Gil, E. R.; De Burguera, M.; Rivera, A.v.; Maxfield, P. *Acta Crystallogr.* **1977**, *B33*, 578.
(18) Dyck, W.-M.; Dehnicke, K.; Weller, F.; Müller, U. Z. *Anorg. Allg. Chem.* **1980**, *470*, 89.
(19) Wellern, H.-O.; Müller, U. *Chem. Ber.* **1976**, *109*, 3039.
(20) Müller, U.; Dyck, W.-M.; Dehnicke, K. *Z. Anorg. Allg. Chem.* **1980**, *468*, 172.
(21) Kirschbaum, K.; Giolando, D. M. *Acta Crystallogr.* **1992**, *C48*, 1837.
(22) Thorn, D. L.; Nugent, W. A.; Harlow, R. L. *J. Am. Chem. Soc.* **1981**, *103*, 357.

Table 1. Selected Bond Lengths (Å) and Bond Angles (deg) for Compounds **2**−**4**

compd **2**[a]		compd **3**[b]		compd **4**	
Ti(1)−N(4)	1.901(3)	T(1)−N(4)	1.906(5)	Ti(1)−N(6)	1.924(6)
Ti(1)−N(1)	2.075(3)	Ti(1)−N(1)	2.067(5)	Ti(1)−N(4)	1.932(5)
Ti(1)−N(5)	2.311(3)	Ti(1)−N(5)	2.274(5)	Ti(1)−N(5)	1.933(5)
N(1)−N(2)	1.183(4)	N(1)−N(2)	1.197(7)	Ti(1)−N(1)	2.150(5)
N(2)−N(3)	1.135(5)	N(2)−N(3)	1.148(8)	Ti(1)−N(8)	2.296(6)
				Ti(1)−N(7)	2.300(6)
				N(1)−N(2)	1.194(7)
				N(2)−N(3)	1.163(7)
N(4)−Ti(1)−N(4a)	98.0(2)	N(4)−Ti(1)−N(4a)	99.9(3)	N(6)−Ti(1)−N(4)	96.3(2)
N(4)−Ti(1)−N(1)	98.3(1)	N(4)−Ti(1)−N(1)	100.6(2)	N(6)−Ti(1)−N(5)	106.8(2)
N(4)−Ti(1)−N(1a)	93.9(1)	N(4)−Ti(1)−N(1a)	89.0(2)	N(4)−Ti(1)−N(5)	94.8(2)
N(1)−Ti(1)−N(1a)	161.30(2)	N(1)−Ti(1)−N(1a)	165.2(3)	N(6)−Ti(1)−N(1)	92.1(2)
N(4)−Ti(1)−N(5a)	171.3(1)	N(4)−Ti(1)−N(5a)	95.3(2)	N(4)−Ti(1)−N(1)	168.2(3)
N(4)−Ti(1)−N(5)	89.9(1)	N(4)−Ti(1)−N(5)	162.7(2)	N(5)−Ti(1)−N(1)	90.8(2)
N(1)−Ti(1)−N(5a)	84.7(1)	N(1)−Ti(1)−N(5a)	80.1(2)	N(6)−Ti(1)−N(8)	160.3(2)
N(1)−Ti(1)−N(5)	81.3(1)	N(1)−Ti(1)−N(5)	87.9(2)	N(4)−Ti(1)−N(8)	88.6(2)
N(5)−Ti(1)−N(5a)	82.5(2)	N(5)−Ti(1)−N(5a)	71.1(2)	N(5)−Ti(1)−N(8)	91.7(2)
N(2)−N(1)−Ti(1)	133.40(3)	N(2)−N(1)−Ti(1)	132.3(4)	N(1)−Ti(1)−N(8)	80.8(2)
N(3)−N(2)−N(1)	177.50(4)	N(3)−N(2)−N(1)	176.9(7)	N(6)−Ti(1)−N(7)	90.6(2)
				N(4)−Ti(1)−N(7)	91.7(2)
				N(5)−Ti(1)−N(7)	160.5(3)
				N(1)−Ti(1)−N(7)	79.8(2)
				N(8)−Ti(1)−N(7)	70.1(2)
				N(2)−N(1)−Ti(1)	133.7(5)
				N(3)−N(2)−N(1)	177.5(8)

[a] Symmetry transformations used to generate equivalent atoms (a) $-x + 2, y, -z + {}^3/_2$. [b] Symmetry transformations used to generate equivalent atoms (a) $-x + 1, y, -z$.

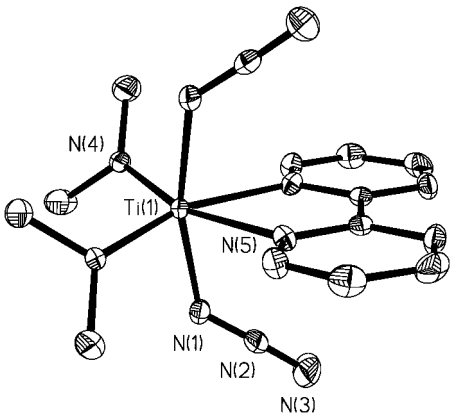

Figure 2. Molecular structure of $[Ti(NMe_2)_2(N_3)_2(bipy)]$ (**3**), showing the atom-numbering scheme. Ellipsoids are drawn at the 30% level. Hydrogen atoms are omitted.

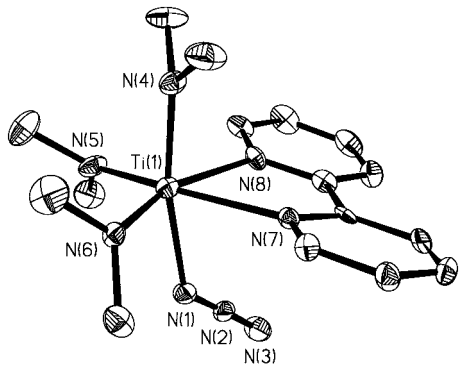

Figure 3. Molecular structure of $[Ti(NMe_2)_3(N_3)(bipy)]$ (**4**), showing the atom-numbering scheme. Ellipsoids are drawn at the 30% level. Hydrogen atoms are omitted.

Scheme 2

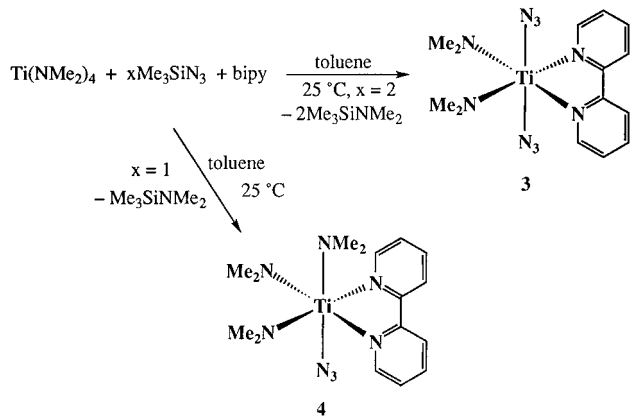

which, in addition, revealed that the solid state consists of monomers with no conspicuously short intermolecular contacts. Overall, the structure of **4** bears a close resemblance to that of **3** but with one of the azide groups replaced by a dimethylamido group. The geometry at titanium is approximately octahedral, and the three dimethylamido groups are arranged in a *mer* fashion. All of the Ti−N bonds in **4** are longer than those in **3**, presumably as a consequence of replacing an azide by a more sterically demanding dimethylamido group. In terms of angles, the major ramification of this replacement is that the equatorial $Me_2N-Ti-NMe_2$ bond angle increases from 99.9(3) to 106.8(2)°. However, the conformation of the azide group with respect to the bipyridyl ligand plane is identical in **3** and **4**.

Film growth experiments on **1** and **2** were carried out in a UHV system consisting of a load lock and growth and analysis chambers. The analysis chamber was equipped with a mass spectrometer and X-ray photoelectron spectrometer with a base pressure maintained at $<5 \times 10^{-10}$ Torr. Film growth from precursor **1** was carried out on a silicon substrate in the temperature range 300−400 °C; the precursor was maintained at a temperature of 90 °C. The Ni:Ti atomic ratio of the resulting TiN film was found to be 1.11. On the basis of XPS, significant quantities of oxygen were not present (<1%); however, the TiN films featured substantial carbon incorporation (∼35%) suggesting the formation of titanium carbonitride rather than titanium nitride. Due to the low volatility of **1** and the

Table 2. Crystal Data, Details of Intensity, Measurement, and Structure Refinement for Compounds **2**−**4**

	2	**3**	**4**
formula	$C_{14}H_{22}N_{10}Ti$	$C_{14}H_{20}N_{10}Ti$	$C_{16}H_{26}N_8Ti$
fw	378.32	376.30	378.35
temp (K)	178(2)	178(2)	153(2)
λ (Å)	0.710 73	0.710 73	0.710 73
crystal syst	orthorhombic	monoclinic	monoclinic
space group	$C222_1$	$I2/a$	$P2/c$
a (Å)	7.120(1)	7.358(2)	15.682(2)
b (Å)	15.899(3)	16.808(4)	8.814(1)
c (Å)	16.946(4)	14.837(6)	15.128(1)
α (deg)	90	90	90
β (deg)	90	95.40(2)	108.39(1)
γ (deg)	90	90	90
V (Å^3)	1918.3(6)	1826.8(1)	1984.2(4)
Z	4	4	4
d(calc) (g/cm^3)	1.310	1.368	1.267
abs. coeff (cm^{-1})	4.65	4.88	4.47
crystal size (mm)	0.46 × 0.40 × 0.23	0.41 × 0.20 × 0.10	0.51 × 0.17 × 0.07
θ range (deg)	2.56−27.49	2.42−22.47	2.69−23.74
tot. no. of rflns	1507	1235	3685
no. of obsd rflns	1451	1188	2241
no. of ref params	119	118	235
GOF on F^2	1.097	1.101	1.037
wR2/R1[a] [$I > 2\sigma(I)$]	0.1055/0.0418	0.1692/0.0671	0.0975/0.0671

[a] $R1 = \sum||F_o| - |F_c||/\sum|F_o|$. $wR2 = [\sum[w(F_o^2 - F_c^2)^2]/\sum[w(F_o^2)^2]]^{1/2}$; $w = 1/[\sigma^2(F_o^2) + (aP)^2 + bP]$, where $P = [\max(0,F_o^2)/3 + 2F_c^2/3]$.

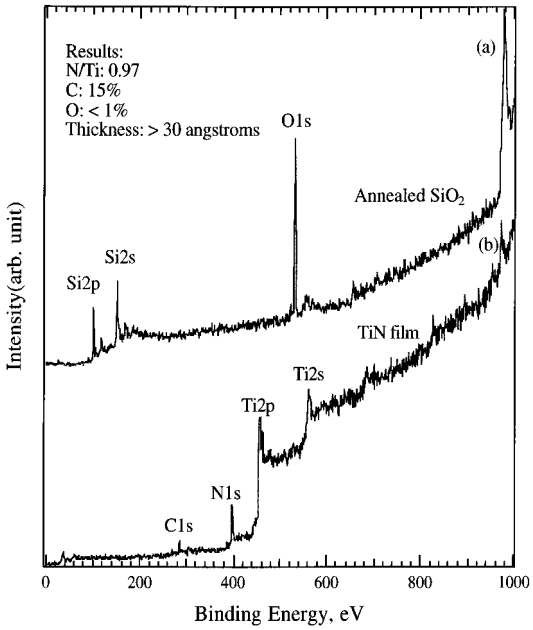

Figure 4. XPS spectra of (a) SiO_2 substrate and (b) TiN film grown from **2** after 10 min at 400 °C.

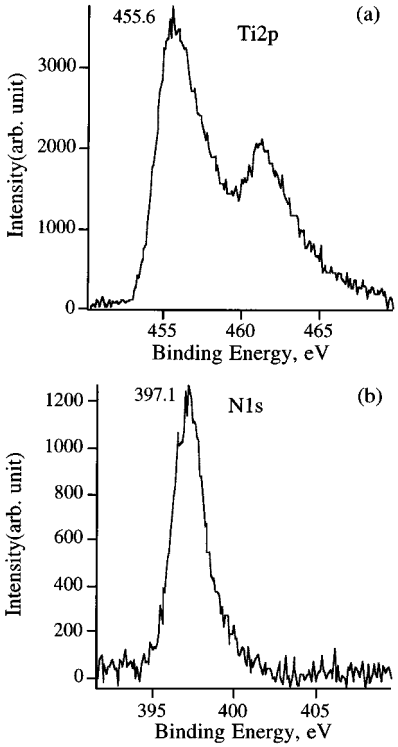

Figure 5. Ti (2p) and N (1s) XPS spectra of TiN film grown from **2** after 10 min at 400 °C.

high carbon content of the resulting film, this compound is considered to be a poor TiN precursor. However, TiN films grown from **2** were distinctly superior. In this case, film growth was carried out on both SiO_2 and nickel substrates in the temperature range 300−400 °C. Interestingly, the quality of the TiN film was found to depend on the precursor temperature. Thus, upon increase of the precursor temperature from 25 to 90 °C the N:Ti atom ratio was found to increase from 0.85 to 0.97; moreover the rate of deposition doubled in this same temperature increment. It is also of interest to note that no film growth was observed from **1** if the precursor temperature was less than 90 °C. Figure 4 shows the XPS spectra of a TiN film grown from **2** with a substrate temperature of 400 °C and a precursor temperature of 90 °C. Figure 5 shows the Ti 2p and N 1s portion of the XPS spectrum with a Ti $2p_{3/2}$ peak present at 455.6 eV and a N 1s peak present at 397.1 eV, consistent with values found in the literature.[23] Significant quantities of oxygen were not detected (<1%); however the as-grown films typically featured ∼10% of carbon. Parenthetically, it is worth mentioning that the amount of carbon contamination in TiN films grown from **2** is less than that reported from other precursors, such as $Ti(NMe_2)_4$.[6]

In summary, a new type of TiN single-source precursor has been developed which features amido and azide groups. At this point, it is not clear whether the source of nitrogen that is being incorporated into TiN is the N_3 or Me_2N ligand.

(23) Zhu, X.-Y.; Wolf, M.; Huett, T.; White, J. M. *J. Chem. Phys.* **1992**, *97*, 5856. Moulder, J. F.; Stickle, W. F.; Sobol, P. E.; Bomben, K. D. *Handbook of X-ray Photoelectron Spectroscopy*; Physical Electronics, Inc.: 1995.

Experimental Section

General Procedures. All manipulations were performed under a dry, oxygen-free dinitrogen atmosphere using standard Schlenk techniques or a HE-493 Vacuum Atmospheres drybox. All solvents were distilled from appropriate drying agents immediately prior to use (sodium for hexanes and toluene; molecular sieves for pyridine). 2,2′-Dipyridyl was procured commercially and used without further purification; Me_3SiN_3 and TMEDA were dried over molecular sieves. Despite the apparent stability of compounds **1**−**4**, *extreme care should be exercised in handling all transition metal azides*. The authors are grateful to Advanced Delivery & Chemical Systems, Inc., for a sample of $Ti(NMe_2)_4$ which was used without further purification. Elemental analyses were performed by Atlantic Microlab, Inc., Norcross, GA.

Physical Measurements. Mass spectra (CIMS) were run on a MAT 4023 instrument, and NMR spectra were recorded on a GE QE-300 spectrometer (^{1}H, 300.19 MHz; ^{13}C, 75.48 MHz). NMR spectra were referenced to either C_6D_6 (which was dried over sodium−potassium alloy and distilled prior to use) or CD_2Cl_2 (which was dried over molecular sieves). ^{1}H and ^{13}C chemical shifts are reported relative to $Si(CH_3)_4$ (0.00 ppm). Melting points were obtained in sealed glass capillaries under argon (1 atm) and are uncorrected.

Preparations. Compound 1. Me_3SiN_3 (1.14 mL, 8.56 mmol) was added dropwise to a yellow solution of $Ti(NMe_2)_4$ (1 mL, 4.28 mmol) in toluene (40 mL) at room temperature. The solution turned blood red after a few minutes and was allowed to stir overnight. After this time the volume of the reaction mixture was reduced to 10 mL and an overlayer of hexanes (25 mL) was added carefully. Solvent diffusion over a period of days at −20 °C afforded 0.840 g of dark red microcrystalline **1** (60% yield). FTIR: 2071.80 cm^{-1} (N_3). Anal. Calcd for $C_4H_{12}N_8Ti$: C, 21.83; H, 5.50; N, 50.91. Found: C, 21.20; H, 5.19; N, 49.99. CIMS (CH_4) (*m*/*e*): calcd mass for $C_4H_{12}N_8Ti$ 221.074264; found 221.074473. No satisfactory NMR data were obtained due to the insolubility of **1** in most solvents.

Compound 2. Me_3SiN_3 (1.14 mL, 8.56 mmol) was added dropwise to a yellow solution of $Ti(NMe_2)_4$ (1 mL, 4.28 mmol) in pyridine (40 mL) at room temperature. The solution, which turned blood red immediately, was allowed to stir for 1 h. After this time the volume of the reaction mixture was reduced to approximately 10 mL and an overlayer of hexanes (25 mL) was added carefully. Solvent diffusion over a period of days at −20 °C afforded 1.14 g of dark red crystals of **2** (70% yield), mp 68−72 °C. ^{1}H NMR (300.15 MHz, C_6D_6)): δ 3.10 (s, 12H, NCH_3), 6.58 (t, 4H, *m*-C_5H_5N), 6.88 (t, 2H, *p*-C_5H_5N), 8.44 (d, 4H, *o*-C_5H_5N). ^{13}C{^{1}H}NMR (75.14 MHz, C_6D_6)): δ 43.98 (N−CH_3), 123.85 (*m*-C_5H_5N), 136.42 (*p*-C_5H_5N), 150.15 (*o*-C_5H_5N). FTIR: 2075.12 cm^{-1} (N_3). Anal. Calcd for $C_{14}H_{22}N_{10}Ti$: C, 44.45; H, 5.86; N, 37.03. Found: C, 44.38; H, 5.94; N, 36.11.

Compound 3. bipy (0.535 g, 3.43 mmol) was added to a yellow solution of $Ti(NMe_2)_4$ (0.8 mL, 3.43 mmol) in toluene (40 mL) at room temperature resulting in an orange colored solution. The dropwise addition of Me_3SiN_3 (0.9 mL, 6.85 mmol) to the foregoing solution resulted in an immediate blood red coloration. After the reaction mixture was stirred for 1 h, the volume was reduced to approximately 20 mL. Cooling of this solution to −20 °C overnight afforded a 55% yield of brown crystalline **3** (mp 80−82 °C). ^{1}H NMR (300.15 MHz, C_6D_6): δ 3.09 (s, 12H, NCH_3), 6.54−8.73 (m, 8H, $C_{10}H_8N$). ^{13}C{^{1}H}-NMR (75.14 MHz, C_6D_6): δ 48.57 (N−CH_3), 121.70 (s, CH, $C_{10}H_8N_2$), 124.05 (s, CH, $C_{10}H_8N_2$), 126.90 (s, CH, $C_{10}H_8N_2$), 136.58 (s, CH, $C_{10}H_8N_2$), 150.17 (s, C, $C_{10}H_8N_2$). FTIR: 2079.52 cm^{-1} (N_3). Anal. Calcd for $C_{14}H_{20}N_{10}Ti$: C, 44.66; H, 5.36; N, 37.23. Found: C, 44.99; H, 4.90; N, 37.16.

Compound 4. bipy (0.588 g, 3.77 mmol) was added to a solution of $Ti(NMe_2)_4$ (0.9 mL, 3.77 mmol) in toluene (40 mL) at room temperature resulting in a color change from yellow to orange. Me_3SiN_3 (0.5 mL, 3.77 mmol) was added dropwise, and the solution turned blood red immediately. After the reaction mixture was stirred for 1 h, the volume was reduced to a total volume of approximately 20 mL. Cooling of this solution to −20 °C overnight afforded a 60% yield of red crystalline **4** (mp 82−84 °C). ^{1}H NMR (300.15 MHz, C_6D_6)): δ 3.04 (s, 18H, NCH_3), 7.34−8.68 (m, 8H, $C_{10}H_8N_2$). ^{13}C{^{1}H} NMR (75.14 MHz, C_6D_6)): δ 43.97 (N−CH_3), 121.29 (s, CH, $C_{10}H_8N_2$), 124.27 (s, CH, $C_{10}H_8N_2$), 126.60 (s, CH, $C_{10}H_8N_2$), 137.36 (s, CH, $C_{10}H_8N_2$), 149.67 (s, C, $C_{10}H_8N_2$). FTIR: 2060.10 cm^{-1} (N_3). Anal. Calcd for $C_{14}H_{20}N_{10}Ti$: C, 50.80; H, 6.93; N, 29.62. Found: C, 49.97; H, 5.93; N, 29.38.

X-ray Crystallography. Crystallographic data and details of the data collection procedures and structure refinement for **2**−**4** are presented in Table 2. Crystals of **2** were grown by solvent diffusion of pyridine and hexanes at −20 °C, whereas **3** and **4** were grown from toluene solutions stored at −20 °C. Data were collected on a Siemens P4 diffractometer at −100 °C with graphite-monochromated Mo Kα radiation (λ = 0.710 73 Å). Accurate unit cell parameters were determined by recentering 25 optimal high-angle reflections. Three standard reflections were measured 4 in every 96 reflections during data collection, and no decrease in intensities was noted. Corrections were applied for Lorentz−polarization and absorption (SHELXA for **4**; face-indexed for **2**) effects. The structures were solved for the heavy atoms by a patterson lamp. Subsequent difference syntheses gave all other non-hydrogen atomic positions, and these were refined by full-matrix least squares on F^2 using the Siemens SHELXL PLUS 5.0 (PC) software package.[24] All non-hydrogen atoms were allowed anisotropic thermal motion. Hydrogen atoms were included at calculated positions (C−H 0.96 Å) and were refined using a riding model and a general isotropic thermal parameter. The final values of atomic positional parameters for **2**−**4** are available in the Supporting Information.

Film Growth. Film growth experiments using precursors **1** and **2** were carried out in a UHV system consisting of a load lock and growth and analysis chambers. The analysis chamber was equipped with a mass spectrometer and X-ray photoelectron spectrometer with the base pressure maintained at $<5 \times 10^{-10}$ Torr. The substrate was mounted on a pedestal which was capable of being transferred between the chambers. In the growth chamber, the heating stage employed a light bulb as the heating source and was enclosed by a copper housing which featured an attached thermocouple. In order to minimize radiation loss the heating stage was surrounded by a quartz tube coated with gold thus permitting deposition temperatures up to 700 °C.

Acknowledgment. Dr. Vincent Lynch of the departmental crystallography laboratory at The University of Texas at Austin is thanked for the low-temperature data collection for **2**−**4**. We are grateful to the Science and Technology Center Program of the National Science Foundation (Grant CHE-08920120), the National Science Foundation (Grant CHE-9629088), and the Robert A. Welch Foundation for generous financial support. A.H.C. is grateful to the Alexander von Humboldt Foundation for a senior research award.

Supporting Information Available: X-ray crystallographic files, in CIF format, for complexes **2**−**4** are available on the Internet only. Access information is given on any current masthead page.

IC9614834

(24) Sheldrick, G. M. *SHELXTL PC Version 5.0*; Siemens Analytical X-ray Instruments, Inc.: Madison, WI, 1994.